NAIC-ID(RS)T-0696-95

NATIONAL AIR INTELLIGENCE CENTER

HEATING EFFECT OF DF LASER UNSTABLE CAVITY WINDOW AND ITS EFFECT ON FAR-FIELD LIGHT SPOT

by

Chen Jinbao, Liu Zejin, et al.

Approved for public release: distribution unlimited

HUMAN TRANSLATION

NAIC-ID(RS)T-0696-95 15 March 1996

MICROFICHE NR: 96C000249

HEATING EFFECT OF DF LASER UNSTABLE CAVITY WINDOW AND ITS EFFECT ON FAR-FIELD LIGHT SPOT

By: Chen Jinbao, Liu Zejin, et al.

English pages: 12

Source: Qiangjiguang Yu Zizishu (High Power Laser and Particle Beams), Vol. 6, Nr. 2, May 1994; pp. 243-249

Country of origin: China
Translated by: Leo Kanner Associates
F33657-88-D-2188
Requester: NAIC/TATD/Bruce Armstrong
Approved for public release: distribution unlimited.

GRAPHICS DISCLAIMER

All figures, graphics, tables, equations, etc. merged into this translation were extracted from the best quality copy available.

HEATING EFFECT OF DF LASER UNSTABLE-CAVITY WINDOW AND ITS EFFECT ON FAR-FIELD LIGHT SPOT

Chen Jinbao, Liu Zejin, Jiang Zhiping, Lu Qisheng, Zhang Zhenwen, and Zhao Yijun

Department of Applied Physics, National University of Defense Technology, Changsha, Hunan, 410073

ABSTRACT: We calculated the temperature rise and phase change of CaF_2 window of unstable cavity DF lasers. The effects on far-field optical spot with or without beam expanding system were cansidered. The result of numerical calculation is given in this paper.

Key words: unstable cavity, DF lasers, CaF_2 window, heating effect, far-field light spot.

I. Introduction

Earlier, during research on intense laser beam propagation, most attention centered on the laser generation process and on atmospheric effects on laser transmission [1,2]. At present, there have been no studies exclusively on the effect of the laser window on laser transmission. During high-power operation of laser devices, after absorbing laser energy by the output window material, temperature rises and thermal deformation will be generated, thus inducing the corresponding variation of refractivity. Due to multiple factors, a laser beam emitted from a high-power laser device is an inhomogeneous light beam, so the effect on refractivity due to the window heating effect is also

inhomogeneous. After a high-power laser beam passes through the window, its wavefront will have an anomaly. This will affect the far-field light spots.

In the authors' earlier work [3,4], they discussed the heating effect and the nonlinearity effect of window material for stable cavities. In the discussion of these earlier results, the window heating effect has a major effect on the far-field light spot. The difference of the additional phase in the near-field is nearly 2Π; the effect of different focal lengths is not consistent. The present article discusses mainly the effect on the far-field light spot due to the distribution of the additional phase such that a heating effect at the CaF_2 window for a DF laser with an unstable cavity should be induced. Consideration was given to the output properties of the laser device. In the calculations, the linear decrease from upper stream to lower stream is applied for the light intensity distribution.

II. Temperature Rise in Window Material and the Corresponding Phase Variation

In the case of an unstable-state process, in the cylindrical coordinate system, the temperature T of the window material is determined by the equation of thermal conductivity:

$$c\rho \frac{dT}{dt} = k\nabla^2 T + \nabla k \cdot \nabla T + \alpha I \qquad (1)$$

In the equation, c, ρ, k and α are, respectively, specific heat, density, coefficient of thermal conductivity, and coefficient of absorption of the material; t is time and I is laser intensity. In approximate terms, it is held that the laser does not attenuate when transmitting within the window. With respect to the CaF_2 crystal

$$c = 0.87 \ \mathrm{J/g.K}$$
$$\rho = 3.179 \ \mathrm{g/cm^3}$$
$$\alpha = 0.001 \ \mathrm{cm^{-1}}$$
$$k(T) = \frac{2920}{T-8} \ (\mathrm{J/m.s.K})^{[3]}$$

The variation of refractivity n with temperature is: $dn/dT=-7.8\times10^{-6}$ (K^{-1}). Therefore, when the thickness of the window material is L, the phase variation due to temperature increase is: $\Delta\Phi = \frac{2\pi}{\lambda}\Delta n \cdot L$.

III. Effect on Far-field Light Spot Due to Temperature Rise at Window

When the transmission distance is much greater than the window radius, this is called far-field transmission. The far-field light spot can be calculated from diffraction theory. Two situations are considered, as follows:

3.1. System in absence of beam expansion (Fig. 1)

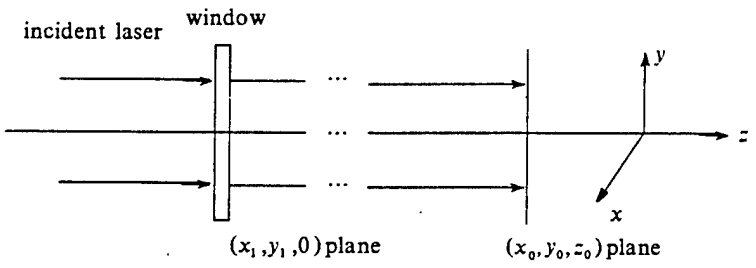

Fig. 1. Laser propagation in absence of beam expansion system

Here, the distribution of the complex vibration amplitude of the far-field light spot is indicated with Fresnel integration

$$u(x_0, y_0) = \frac{\exp(jkz_0)}{j\lambda z_0} \iint_{-\infty}^{\infty} u_0(x_1, y_1) e^{j\Delta\Phi(x_1, y_1)} e^{j\frac{k}{2z_0}[(x_0 - x_1)^2 + (y_0 - y_1)^2]} dx_1 dy_1 \qquad (2)$$

In the equation, $u_0(x_1, y_1)$ is the complex vibration amplitude on the $(x_1, y_1, 0)$ plane without considering the phase variation $\Delta\Phi(x_1, y_1)$ due to rise in temperature.

3.2. System in presence of beam expansion (Fig. 2)

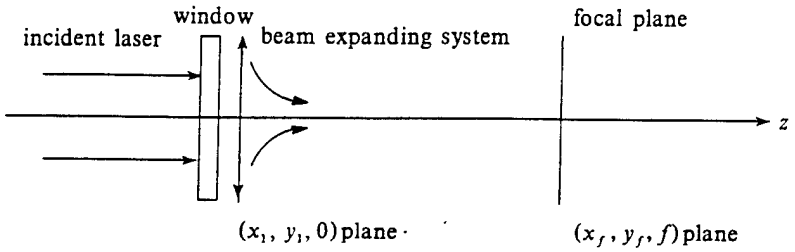

Fig. 2. Laser propagation in presence of beam expansion system

Generally speaking, beam expansion focusing systems are used in the far-field transmission of high-power lasers. Here, an ideal beam expansion focusing system is assumed, and we only introduce a gaussian phase distribution exp .
Here, the light-spot complex vibration amplitude distribution $u(x_f, y_f)$ on the focal plane of the beam expansion system can be expressed with Fraunhofer integration. That is,

$$u(x_f, y_f) = \frac{\exp(jkf)}{j\lambda f} \exp\left[j\frac{k}{2f}(x_f^2 + y_f^2)\right] \iint_{-\infty}^{\infty} u_0(x_1, y_1) e^{j\Delta\Phi(x_1, y_1)} e^{-j\frac{k}{f}(x_1 x_f + y_1 y_f)} dx_1 dy_1 \qquad (3)$$

IV. Selection of Calculation Parameters and Division of Lattice

4.1. Window parameters

The window diameter Φ=60mm, and thickness L=1cm, with metal

The window diameter Φ=60mm, and thickness L=1cm, with metal support.

4.2. Incident laser parameters

The wavelength λ is 3.8μm; the irradiation time is 1s; and there are three power situations: 10^3W, 10^4W, and 10^5W. The light spots are ring-shaped (Fig. 3); the distribution of light intensity (Fig. 4) decreases linearly along the X-axis, but remains constant along the Y-direction. Assume that the laser device in an ideal operating state, and that the output laser beam is a parallel beam, and that the laser phase, when incident at the window, is zero.

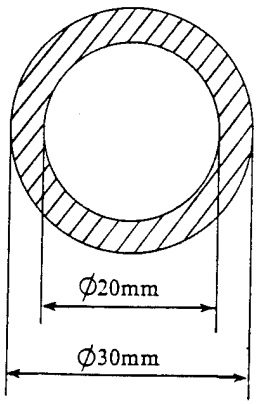

Fig. 3. Light spot of incident laser

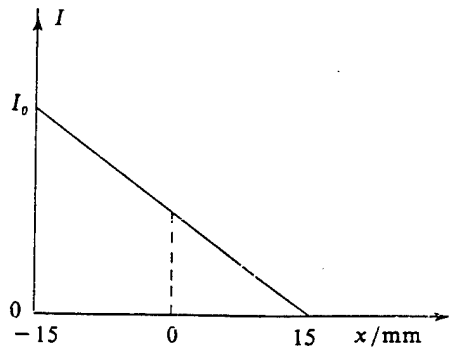

Fig. 4. Distribution of incident laser intensity

4.3. Beam expansion system parameters

The focal length f is 55m. After beam expansion, the internal diameter Φ_1 of the light spot is 80mm, and the outer diameter Φ_2 is 120mm. The light spots are linearly amplified.

4.4. Selection of lattice

and (3), numerical computations of the three equations are made. In the temperature field calculations, the classical difference display format is applied in polar coordinates. Based on the von Neumann stability conditions,

$$a\Delta t\left(\frac{1}{\Delta\rho^2}+\frac{1}{\Delta\theta^2}\right)\leqslant\frac{1}{2}$$

In the equation, $a=c\rho/K$; and $\Delta\rho$ and $\Delta\Theta$ are, respectively, the polar radius and step length of the polar angle. Δt is the time step length. When the lattice points are selected as 60x60, Δt should be smaller than 480μs. In the actual computations, we take Δt as 200μs.

We use Eqs. (2) and (3) for computing the far-field light spots. By converting integration into finite summation, the following condition should be satisfied.

$$|r_1-r_2|\ll\lambda$$

In the equation, r_1 and r_2 are the distances to any point in the plane from two arbitrary points in the same area element.

$$r_1^2=(x_0-x_1)^2+(y_0-y_1)^2+z_0^2$$

$$r_2^2=(x_0-x_2)^2+(y_0-y_2)^2+z_0^2$$

$$|r_2-r_1|\approx\frac{1}{z_0}\left|2x_0(x_1-x_2)+x_2^2-x_1^2\right|$$

$$|r_2-r_1|\leqslant\frac{1}{z_0}\left|2x_0(x_1-x_2)\right|_{max}+\frac{1}{z_0}\left|x_2^2-x_1^2\right|_{max}$$

In our computations, when z_0-50m, we have
Therefore, the computational process is stable.

V. Calculation Results and Discussion

5.1. Temperature rise at window and induced phase variation

Fig. 5 is an isopleth diagram and a three-dimensional diagram for temperature rise distribution at the window when the DF laser power is 1kW and the irradiation time is 1s. The maximum temperature rise is 0.4086K; Fig. 6 indicates the corresponding phase variation of the wavefront. The maximum phase variation is -0.0527rad. When the DF laser power is 10^4W and 10^5W, the variation distribution diagrams for the distribution of variations in the temperature field and in the phase are similar to those when the laser is 10^3W. Only, the maximum temperature rise values are 4.074K and 40.87K, and the maximum phase variation values are, respectively, -0.5254rad and -5.2067rad. The temperature rise is almost proportional to laser power; this is because the thermal conductivity coefficient of the CaF_2 crystal is small and its irradiation time is short.

5.2. Far-field light spots in presence of beam expansion system

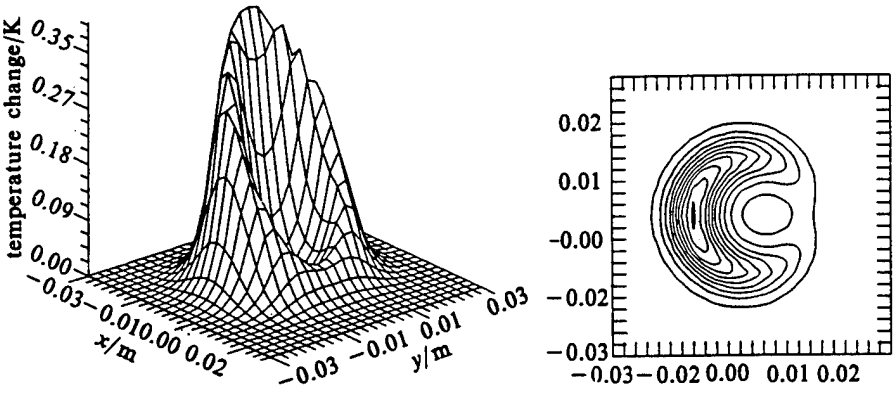

Fig. 5. Temperature rise of CaF_2 window caused by laser

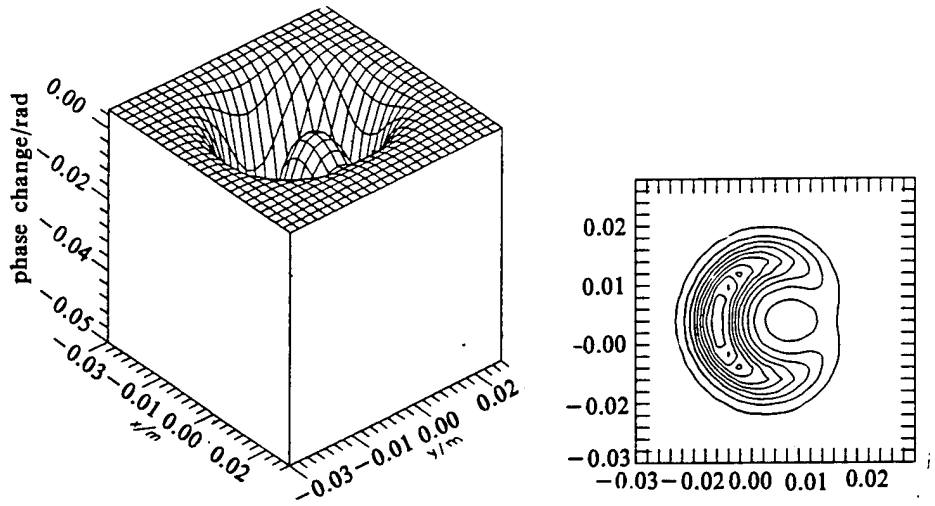

Fig. 6. Phase change caused by temperature rise

Fig. 7 indicates the distribution of light intensity (there are the same shapes in the figures for laser power for 10^3W, 10^4W and 10^5W) on the focal plane when there is phase variation induced by the temperature rise, but not considering the CaF_2 window material. The isopleth diagram shows a somewhat squarish

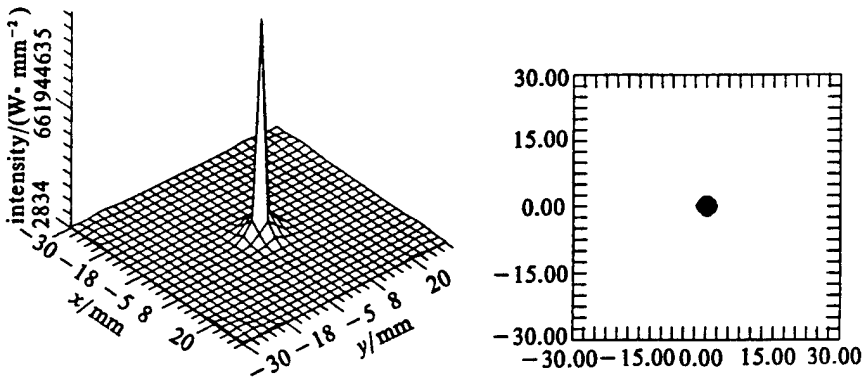

Fig. 7. Distribution of light intensity on focal plane without considering phase change caused by temperature rise

appearance, not circular. This is because of the limited number of lattice points in the numerical calculation, so that these limited number of data do not provide smoothly plotted curves. After considering the phase variation and the laser powers at 10^3 and 10^4W, the light intensity distribution at the focal plane is close to that in Fig. 7. However, since the laser power is 10^5W, the light intensity distribution on the focal plane is as shown in Fig. 8.

From the foregoing, when a beam expansion system is present, in the case of wavefront phase variation with laser power at 10^3W and 10^4W, there is little effect on the far-field light spots. However, when the laser power is 10^5W, the wavefront phase variation has greater effect on far-field light spots. In this case, the light spot area grows larger and the light beam is diverted. We also can see from the data in our calculations, that there is a deviation at the center of the light spot, and

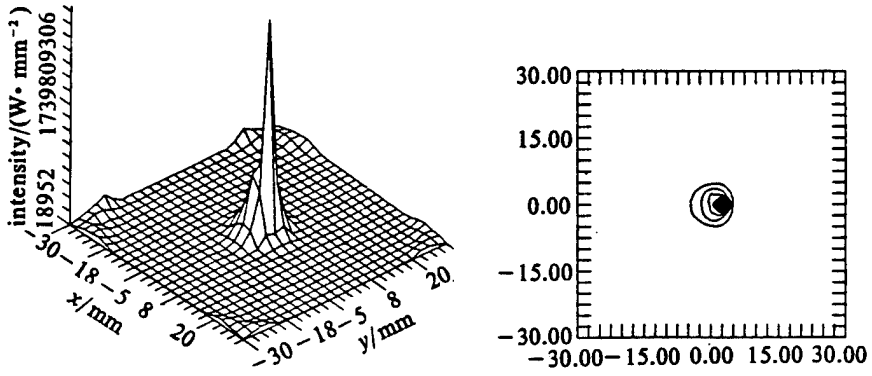

Fig. 8. Distribution of light intensity on focal plane when allowance is made for phase change caused by temperature rise for laser power of 10^5W

the maximum value of light intensity is about 1mm deviation from the center.

5.3. Far-field light spots when there beam expansion system is not present

Fig. 9 indicates the light intensity distribution at z=100m when the wavefront phase variation is not considered. After allowing for wavefront phase variation, when the laser power is 10^3W, the corresponding light intensity distribution does not differ markedly from Fig. 9. Fig. 10 indicates the corresponding diagram shape when laser power is 10^4W. Fig. 11 indicates the corresponding diagram shape when laser power is 10^5W. Here, the light-spot center deviates from the original position by 10mm. Upon comparing Fig. 11 with Fig. 9, the light-spot area grows larger along with appreciable image aberration and coma aberrations.

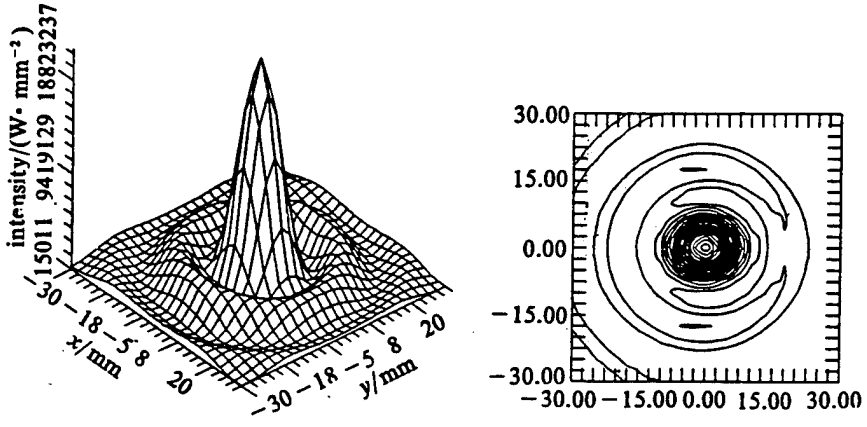

Fig. 9. Far-field light spot without allowing for phase change, in absence of beam expansion system

We can see that in the case of the absence of a beam expansion system, greater effect will be seen on the far-field light spot when the laser power exceeds 10^4W, thus seriously damaging light-beam quality. The laser output passes through the window opening, inducing a temperature rise in material at the window opening, thus inducing a wavefront phase variation in the laser. At high powers, a greater effect is exercised on the far-field light spot, thus being disadvantageous to long-distance laser beam transmission. This article presents many quantitative and direct results. Some of the results were observed in the authors' experiments, including the positional drift and phase variation of the far-field light spot center, and image aberration exhibited in the far-field light-spot distribution.

The authors express their gratitude for support given to the research from work units, including the Handan Institute of Purification Equipment.

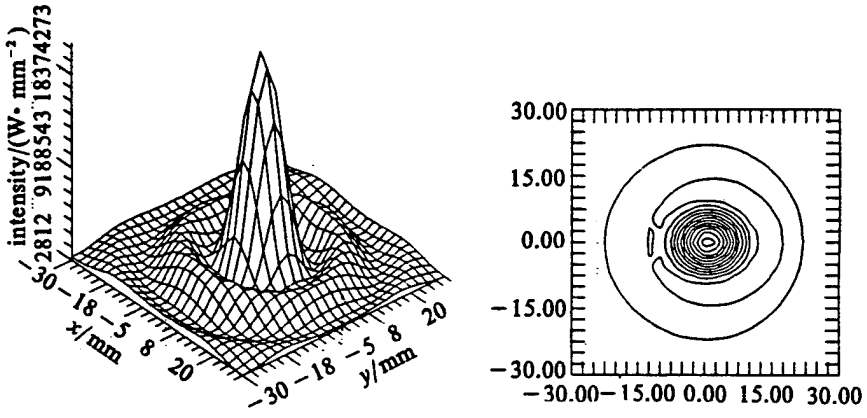

Fig. 10. Far-field light spot, with allowance made for phase change, at laser power 10^4W

The first draft of the article was received on March 22, 1993; the final revised draft was received on January 3, 1994.

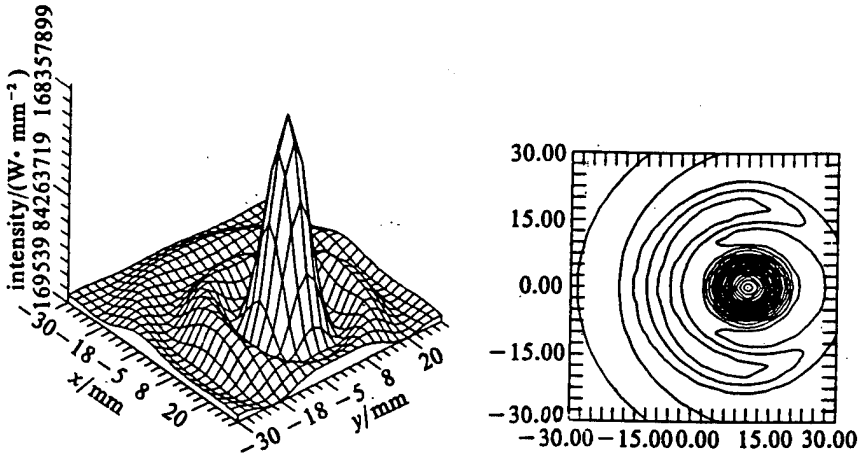

Fig. 11. Far-field light spot, allowing for the phase change, laser power 10^5W

DISTRIBUTION LIST

DISTRIBUTION DIRECT TO RECIPIENT

ORGANIZATION	MICROFICHE
B085 DIA/RTS-2FI	1
C509 BALL0C509 BALLISTIC RES LAB	1
C510 R&T LABS/AVEADCOM	1
C513 ARRADCOM	1
C535 AVRADCOM/TSARCOM	1
C539 TRASANA	1
Q592 FSTC	4
Q619 MSIC REDSTONE	1
Q008 NTIC	1
Q043 AFMIC-IS	1
E404 AEDC/DOF	1
E410 AFDTC/IN	1
E429 SD/IND	1
P005 DOE/ISA/DDI	1
1051 AFIT/LDE	1
P090 NSA/CDB	1

Microfiche Nbr: FTD96C000249
NAIC-ID(RS)T-0696-95